European Polymer Journal 45 (2009) 2858–2866

Contents lists available at ScienceDirect

European Polymer Journal

journal homepage: www.elsevier.com/locate/europolj

# Hydrophilic poly(ethylene oxide)–aramide segmented block copolymers

A. Arun [a,b,1], R.J. Gaymans [a,*]

[a] Faculty of Science and Technology, University of Twente, P.O. Box 217, 7500 AE Enschede, The Netherlands
[b] Dutch Polymer Institute, P.O. Box 902, 5600 AX Eindhoven, The Netherlands

ARTICLE INFO

*Article history:*
Received 19 May 2009
Received in revised form 26 June 2009
Accepted 1 July 2009
Available online 10 July 2009

*Keywords:*
Segmented block copolymer
Aramide
Monodisperse
Poly(ethylene oxide)
Poly(propylene oxide)

ABSTRACT

The present paper discusses block copolymers with segments of either poly(ethylene oxide), poly(propylene oxide), or mixtures of poly(ethylene oxide)/poly(propylene oxide) and monodisperse aramide segments. The length of the polyether segments as well as the concentration of polyethylene oxide was varied. The synthesized copolymers were analyzed by DSC, FTIR, AFM and DMTA. In addition, the hydrophilicity was studied.

The crystallinity of the monodisperse aramide segments was found to be high and the crystals, dispersed in the polyether phase, displayed a nano-ribbon morphology. The PEO segments were able to crystallize and this crystalline phase reduced the low-temperature flexibility. The PEO crystallinity and melting temperature could be strongly reduced by copolymerization with PPO segments. By using mixtures of PEO and PPO segments, hydrophilic copolymers with decent low-temperature properties could be obtained.



## 1. Introduction

Segmented block copolymers comprise alternating flexible and crystallizable rigid segments [1,2]. The rigid segments crystallize into nano ribbons dispersed in the amorphous matrix and act as physical crosslinks and as reinforcing fillers for the amorphous matrix. The rigid segments provide the copolymer with dimensional and thermal stability while the flexible segments give the material elasticity. Polyethers are often used as flexible segments due to their low glass transition temperature and their good tensile properties.

Hydrophilic segmented block copolymers can be obtained with poly(ethylene oxide) (PEO) segments and such copolymers find applications in numerous fields, including industries for textile, packaging material, construction and gas separation. For several of these applications, the low-temperature properties are crucial. Hydrophilic segmented block copolymers have also gained increasing attention for biomedical applications such as drug delivery systems, contact lenses, catheters and wound dressings.

Several PEO-based segmented block copolymers with rigid segments constituted of either urethanes [3–6], esters [7–9] or amides [10–13] have been reported on. PEO segments demonstrate a low glass transition temperature ($\sim -40\,^{\circ}C$) and can easily undergo crystallization. Moreover, increasing the PEO length gives rise to a higher PEO melting temperature and a higher crystallinity [12]. PEO-containing segmented block copolymers have low contact angles with water [14,15], a high water vapor transport [16] and a high selective $CO_2$ transport [10,11,17]. However, the crystalline PEO phase reduces the low-temperature flexibility [12].

The use of hydrophilic PEO segments results in a strong increase in water absorption of the copolymers [17,18]. As the water absorption increases the tensile properties of PEO-based copolymers are reduced, mainly as a result of swelling [18,19]. The swelling of the material can be controlled by employing mixtures of hydrophilic (PEO) and hydrophobic soft segments, poly(tetramethylene oxide) (PTMO) or poly(propylene oxide) (PPO) [3,13,20–22]. The properties of copolymers with mixtures of hydrophilic PEO and hydrophobic PTMO blocks have been studied

* Corresponding author. Tel.: +31 534892970.
*E-mail address:* r.j.gaymans@utwente.nl (R.J. Gaymans).
[1] Presently at Government Arts College, Tiruvannamalai, Tamil Nadu, India.

0014-3057/$ - see front matter © 2009 Elsevier Ltd. All rights reserved.
doi:10.1016/j.eurpolymj.2009.07.002

[13,20,21,23], and the crystalline melting temperature of the PEO segments was found to decrease with increasing PTMO concentration [23]. The PTMO segments thus disturbed the crystallization of their PEO counterparts, however, without this leading to a fully amorphous polyether phase.

Poly(propylene oxide) (PPO) segments have methyl side groups that hinder the crystallization. Moreover, copolymers with PPO segments have a low glass transition temperature (−65 °C), excellent low-temperature properties [24]. The copolymers with PPO segments, as compared to with PEO segments, are also much less hydrophilic as a result of the lower ether group concentration. The rigid segments in block copolymers often have a low crystallinity and part of the non-crystallized rigid segments is dissolved in the amorphous phase. A fast and more complete crystallization of the rigid segments can be obtained by using crystalline segments of monodisperse length [13,24–28].

Segmented block copolymers with monodisperse aramide (TΦT) and PTMO segments have been well studied [2,29–32]. Monodisperse aramide segments have been found to crystallize fast, display a relatively high modulus and an almost temperature-independent rubbery plateau. A copolymer of the TΦT–aramide with PEO has briefly been mentioned [29] and copolymers of PPO–TΦT have so far not been reported on. Di-aramide with very short PEO units (88–132 g/mol) have been synthesized and had very high melting temperatures (416 °C) [33,34]. Also have been studied PEO–aramide diblock copolymers [35,36]. It would thus be interesting to accomplish a significant reduction in the PEO crystallinity while still maintaining a hydrophilic copolymer. In this respect the use of the amorphous PPO as second segment might be more suitable than the semi-crystalline PTMO.

This article describes the synthesis and a selection of properties of segmented block copolymers based hydrophilic PEO and hydrophobic PPO segments. Fig. 1 displays the chemical structures of the segments used in the block copolymers. The employed PPO segment was end-functionalized with PEO units to give rise to a higher reactivity (PEO–PPO–PEO).

The used hard segments (HS) were comprised of bisesterdiamide TΦT units that were monodisperse in length (Fig. 1). These copolymers were denoted as $PEO_x/PPO_z$–TΦT, where $x$ and $z$ represent the PEO and PPO molecular weights, respectively. The influence of the polyether phase composition on the low-temperature transitions, low-temperature flexibility and the copolymer hydrophilicity was studied. Moreover, the aramide crystallinity and melting temperatures were investigated as functions of the polyether compositions. It was deemed particularly interesting to determine whether, for a certain hydrophilicity, the low-temperature properties could be improved by using mixtures of PEO and PPO segments.

## 2. Experimental section

### 2.1. Materials

*p*-Phenylenediamine (PPA), *N*-methyl-2-pyrrolidone (NMP), phenol, dichloromethane and three grades of poly(ethylene oxide) (i.e., with an $M_n$ of 1000, 1500 and 2000 g/mol) were obtained from Aldrich. The polyethers were denoted $PEO_{1000}$, $PEO_{1500}$ and $PEO_{2000}$. Moreover, three grades of difunctional poly(propylene oxide) end-capped with 20 wt.% ethylene oxide (EO–PPO–EO), i.e., Acclaim polymers with an $M_n$ of 2200, 4200 and 6300 g/mol, were obtained from Bayer AG, Germany, and denoted $PPO_{2200}$, $PPO_{4200}$ and $PPO_{6300}$. Tetra-isopropyl orthotitanate (Ti($i$-$OC_3H_7)_4$) was obtained from Aldrich and diluted in *m*-xylene (0.05 M) received from Fluka. Irganox 1330 was obtained from CIBA, and methyl-(4-chlorocarbonyl)benzoate (MCCB) was obtained from Dalian (China). The synthesis of the di-aramide units, TΦT-dimethyl, have been described elsewhere [29,31].

### 2.2. Synthesis of the segmented block copolymers

Monodisperse polyamide block copolymers were synthesized by a polycondensation reaction using polyether segments and monodisperse TΦT-dimethyl aramide hard segments. The synthesis of $PEO_{2000}$–TΦT is here given as an example. The reaction was carried out in a 250-ml stainless steel vessel with a nitrogen inlet and mechanical stirrer. The vessel, containing TΦT-dimethyl (4.70 g, 0.01 mol), $PEO_{2000}$ (20 g, 0.01 mol), Irganox 1330 (0.25 g), and 70 mL NMP was heated in an oil bath to 180 °C, after which the catalyst solution was added (2.5 mL of 0.05 M Ti($i$-$OC_3H_7)_4$ in *m*-xylene). The stirred reaction mixture was heated to 180 °C for 30 min and the temperature was subsequently raised step-wise to 250 °C within an hour. The reaction mixture was stirred at 250 °C for 2 h, after which the pressure was carefully reduced ($P$ < 20 mbar) to distil off the NMP. The pressure was further reduced to <0.3 mbar for 1 h, and the reaction mass was then cooled slowly while maintaining the low pressure. The resultant copolymer was transparent

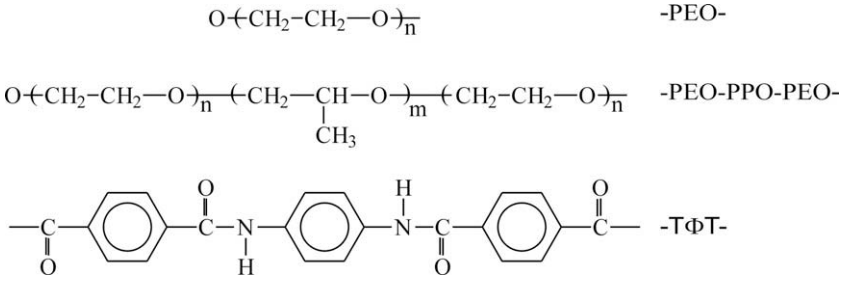


**Fig. 1.** The chemical structures of the –PEO–, –PEO–PPO–PEO– and –TΦT– segments used in the block copolymers.

with a yellowish hue. Before analysis, the polymer was dried in a vacuum oven at 70 °C for 24 h.

### 2.3. Viscometry

Viscometry was used to examine the molecular weights of the obtained polymers. Values of inherent viscosity ($\eta_{inh}$) were determined at 25 °C using a capillary Ubbelohde type 0B viscometer. The polymer solution had a concentration of 0.1 g/dL in a 1:1 (molar ratio) mixture of phenol/1,1,2,2-tetrachloroethane.

### 2.4. Atomic force microscopy (AFM)

AFM measurements were carried out with a nanoscope IV controller (Veeco) operating in tapping mode. The AFM was equipped with a J-scanner with a maximum size of 200 μm$^2$. A TESP-cantilever (Veeco) was used and gentle tapping was applied to obtain the phase images. The amplitude in free oscillation was 5.0 V, and the operating set point value ($A/A_o$) was chosen to the relatively low value of 0.7. Scan sizes were 1–3 μm$^2$ in order to obtain the best possible contrast. Solvent cast samples, approx. 20 μm thick, were prepared from a 3 wt.% solution in HFIP on a silicon wafer and subjected to the AFM analysis. No heat treatment was given to the films.

### 2.5. Differential scanning calorimetry (DSC)

DSC was used to determine the melting and crystallization temperatures and enthalpies of the polyether block copolymers. Thermograms were recorded on a Perkin-Elmer DSC7 apparatus, equipped with a PE7700 computer and TAS-7 software. All samples were dried in a vacuum oven at 70 °C overnight before use. Dried samples (8–12 mg) were heated from −50 °C to approximately 30 °C above the melting temperature, and subsequently cooled and heated again at a rate of 20 °C/min. The maximum of the endothermic peak in the second heating scan was used to determine the melting temperature ($T_m$).

### 2.6. Fourier transform infrared (FTIR) spectroscopy

FTIR was used to determine hard segment crystallinity. Infrared spectra were obtained with a Biorad FTS-60 spectrometer with a resolution of 4 cm$^{-1}$. The measurements were carried out at room temperature on samples prepared by adding a droplet of the block copolymers in solution (HFIP (1 g/L) on a pressed KBr pellet. After evaporation of the solvent, a thin polymer film remained on the pellet, on which the analysis was performed. The degree of crystallinity of the rigid segments in the polymers ($X_c$) could be estimated by using Eq. (1).

$$X_{c,FTIR} = \frac{\text{Crystalline amide peak}}{\text{Amorphous} + \text{crystalline amide peak}} = \frac{\lambda_{25\ ^\circ C(1647\ cm^{-1})}}{a \times \lambda_{25\ ^\circ C(1674\ cm^{-1})} + \lambda_{25\ ^\circ C(1647\ cm^{-1})}} \quad (1)$$

The heights of the amorphous and crystalline amide peaks were related by the factor '$a$' with a value of 2.4 [28].

### 2.7. Dynamic mechanical thermal analysis (DMTA)

The torsion behavior (storage modulus G′ and loss modulus G″ as functions of temperature) was measured using a Myrenne ATM3 torsion pendulum at a frequency of 1 Hz and 0.1% strain. Before use, injection molded polymer samples (70 × 9 × 2 mm$^3$) were dried in a vacuum oven at 50 °C overnight. Following this, samples were cooled to −100 °C and subsequently heated at a rate of 1 °C/min. The glass transition temperature ($T_g$) was defined as the maximum of the loss modulus, and the flow temperature ($T_{flow}$) was determined as the temperature where the storage modulus reached 0.5 MPa. The temperature at which the rubber plateau started was denoted as the flex temperature ($T_{flex}$) and the storage modulus at 20 and 50 °C were labeled $G'_{20\ ^\circ C}$ and $G'_{50\ ^\circ C}$.

### 2.8. Water absorption

The equilibrium water absorption (WA) was measured on pieces of injection-molded polymer bars. The samples were placed in a desiccator with a layer of demineralized water for four weeks at room temperature. The water absorption was defined as the weight gain of the polymer according to Eq. (2):

$$\text{Water absorption} = \frac{m - m_0}{m_0} \times 100\%[wt.\%] \quad (2)$$

where $m_0$ is the weight of the dry sample and $m$ the weight of the sample after conditioning to equilibrium.

## 3. Results and discussion

A series of copolymers with aramide (TΦT) hard segments and PEO and PPO soft segments was studied. The hydrophilicity of the copolymers was modified by varying the polyether segment length and also by using mixtures of PEO and PPO segments. The TΦT-dimethyl unit, monodisperse in length, was prepared prior the polymer synthesis. The poly(propylene oxide) had EO end-groups (EO–PPO–EO) and this EO content was 20 wt.%. The primary alcohols of the EO end-groups were more reactive than their secondary counterparts in PPO, for which reason the end-groups and EO–PPO–EO segments were suitable for preparing high molecular weight copolymers. The EO–PPO–EO segments were denoted PPO.

### 3.1. Materials

The copolymers were synthesized starting from TΦT-dimethyl ester and dihydroxy PEO and PPO segments using a high-temperature melt polymerization. As TΦT is a short unit (314 g/mol), its concentration in the copolymers was low - ranging from 23 down to 5 wt.%. For the calculations of the concentration of the TΦT segment, the employed molecular weight was that of the segment without ester units. This was due to the fact that the ester units have been found not to take part in the crystallization [30]. Even at these low TΦT concentrations, the materials were in the solid state. The inherent viscosities of the material were ⩾1.0 dL/g indicating a successful formation of high

**Table 1**
Selected properties of the $PEO_x$/EO–PPO–$EO_y$–TΦT block copolymers.

| Polymer | PEO/PPO (mol ratio) | HS [wt.%] | PEO | | $\eta_{inh}$ (dl/g) | DSC | | | | DMA | | | | | FTIR | WA [%] |
|---|---|---|---|---|---|---|---|---|---|---|---|---|---|---|---|---|
| | | | Copol [wt.%] | SS[a] (mol%) | | PEO | | TΦT | | $T_g$ [°C] | $T_{flex}$ [°C] | $T_{m,TΦT}$ [°C] | G′ (20 °C) [MPa] | G′ (50 °C) [MPa] | $X_{c,TΦT}$ (%) | |
| | | | | | | $T_m$ | $\Delta H_{m,PEO}$ | $T_m$ | $\Delta H_m$ | | | | | | | |
| $PEO_{1000}$ | 100/0 | 22.4 | 77.6 | 100 | 1.4 | −8 | 14 | 120 | 33 | −42 | −19 | 145 | 29 | 28 | 67 | 64 |
| $PEO_{1500}$ | 100/0 | 16.5 | 85.5 | 100 | 1.5 | 27 | 32 | nm | nm | −38 | 25 | 100 | 14 | 5 | 41 | 103 |
| $PEO_{2000}$ | 100/0 | 13.1 | 86.9 | 100 | 2.0 | 35 | 64 | nm | nm | −41 | 35 | 70 | 79 | 1 | 21 | 125 |
| $PEO_{2000}/PPO_{2200}$ | 75/25 | 12.8 | 69.8 | 81 | 1.6 | 32 | 64 | 96 | 4 | −45 | 35 | 105 | 46 | 6 | 25 | 88 |
| | 50/50 | 12.6 | 52.4 | 59 | 1.7 | 26 | 26 | 111 | 13 | −52 | 35 | 115 | 10 | 5 | 33 | 82 |
| | 25/75 | 12.4 | 34.9 | 40 | 1.6 | – | – | 123 | 28 | −60 | 10 | 135 | 9 | 8 | 57 | 46 |
| $PPO_{2200}$ | 0/100 | 12.1 | 17.6 | 20 | 1.0 | – | – | 135 | 49 | −59 | −47 | 140 | 9 | 10 | 81 | 14 |
| $PPO_{4200}$ | 0/100 | 6.8 | 18.6 | 20 | 1.12 | – | – | nm[b] | nm | −59 | −48 | 100 | 3 | 3 | 59 | 13 |
| $PPO_{6300}$ | 0/100 | 4.7 | 20.9 | 20 | –[a] | – | – | nm | nm | −48 | −45 | 75 | 1.0 | 1.0 | 40 | 20 |

[a] $PPO_{6300}$–TΦT could not be dissolved.
[b] nm, not measurable.

molecular weight copolymers (Table 1). The $PPO_{6300}$–TΦT copolymer swelled but could not be dissolved in the 1:1 (molar ratio) mixture of phenol/1,1,2,2-tetrachloroethane used for the viscosity measurements, which was indicative of the formation of a high molecular weight product.

The polyether phase contained varying amounts of poly(ethylene oxide). The composition of the matrix phase is important for the water absorption, surface properties and the gas transport properties. Thus, in addition to the polyether concentration in the copolymer also the PEO concentration in the ether phase is of considerable relevance and values for these parameters are given in Table 1. PEO has a regular structure and crystallizes easily which led to the copolymers displaying, next to a glass transition temperature also a melting temperature of the PEO segments [12]. On the other hand, PPO is amorphous due to its methyl side groups and the copolymers containing PPO thereby had a low $T_g$ [24]. It was also investigated to which extent the PEO crystallinity and the copolymer hydrophilicity could be changed by varying the copolymer composition.

### 3.2. DSC

The melting behavior of the copolymers was investigated with DSC and the data obtained from the second heating scan were used to exclude the influence of the thermal history of the polymer (Table 1). The melting temperature of the PEO segments increased considerably with an increasing PEO segment length and decreased somewhat with an increasing PPO concentration (Table 1). Also the heat of fusion per weight of PEO increased with the PEO segment length and decreased with the PPO concentration. The copolymers comprised solely of PPO displayed no PPO melting transition. The change in PEO melting temperature and heat of fusion with the PEO segment length in the copolymers could be explained as a result of the changing crosslink density [12].

Some typical DSC thermograms of the PEO/PPO series are presented in Fig. 2.

In the presence of PPO, the PEO heat of fusion decreased to a larger extent than expected and this might have been due to a hindrance of the PPO segments. Although, the presence of PPO lowered the $T_g$ and thus increased the crystallization window. A possible explanation was that the PEO segments, at low concentrations, were not randomly distributed in the phase containing the mixture of PPO/PEO but rather present as dispersed particles. It is known that the crystallization from a finely dispersed phase is much more difficult since not all dispersed particles can be nucleated.

The TΦT melting temperatures were often hard to observe and the heat of fusion values difficult to determine (Fig. 2). This has been seen before and can be ascribed to the low TΦT concentrations [29,31,32]. The $T_m$ of the TΦT segment is known to decrease with an increasing polyether concentration and can be explained by a solvent effect of the polyether segments [29]. At a constant polyether concentration, the $T_m$ of the TΦT in the copolymers also decreased with increasing PEO concentration (Table 1) which suggests that the interaction of TΦT was stronger with PEO as opposed to with PPO and much stronger than with PTMO [29,31,32]. The interaction of TΦT with polyether thus increases in the order PTMO < PPO < PEO.

With an increasing PEO concentration, also the $\Delta H_m$ values of TΦT were lowered. Moreover, a significant reduction

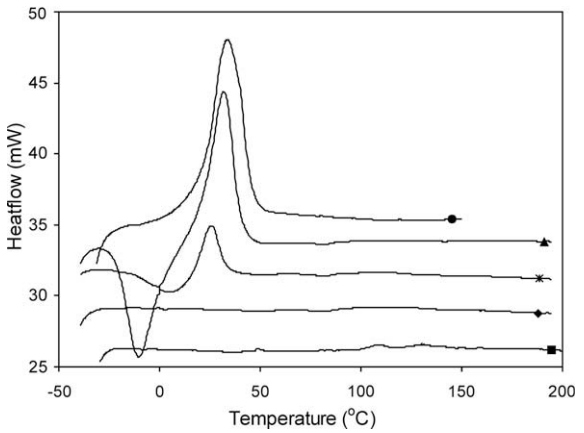


**Fig. 2.** DSC results of the $PEO_{2000}/PPO_{2200}$–TΦT copolymers: ●, $PEO_{2000}$; ▲, $PEO_{2000}/PPO_{2200}$ (75/25); ✳, $PEO_{2000}/PPO_{2200}$ (50/50); ♦, $PEO_{2000}/PPO_{2200}$ (25/75); ■, $PPO_{2200}$.

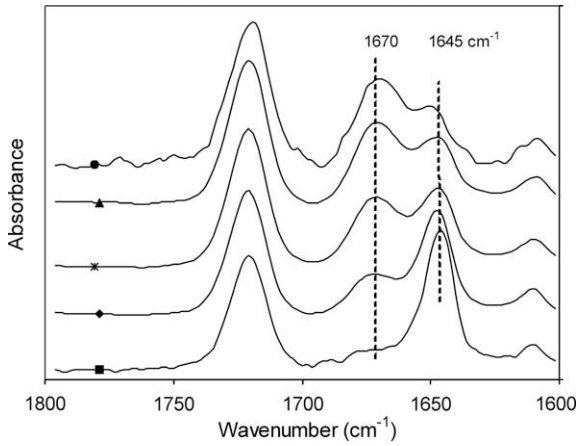


**Fig. 3.** FTIR spectra of the $PEO_{2000}/PPO_{2200}$–TΦT copolymers: ●, $PEO_{2000}$; ▲, $PEO_{2000}/PPO_{2200}$ (75/25); ✳, $PEO_{2000}/PPO_{2200}$ (50/50); ♦, $PEO_{2000}/PPO_{2200}$ (25/75); ■, $PPO_{2200}$.

of the $\Delta H_m$ values could be observed for the PEO–T6T6T copolymers without a lowering of the T6T6T crystallinity. This was explained as the result of a special interaction of PEO and amide segments in the melt [12].

### 3.3. FTIR

A specific method for studying the crystallinity of amide segments in copolymers is by Fourier transform infrared (FTIR) spectroscopy [12,31,32]. The wave number of the amide carbonyl absorbance band is sensitive to the H-bonding strength. For TΦT, in the crystalline state, this occurred at ~1645 $cm^{-1}$ and, in the amorphous state, at 1680–1690 $cm^{-1}$ [31,32]. The wave number of the ester carbonyl band was 1720 $cm^{-1}$ and this ester band was found not to be sensitive to the packing of the chains [12,31,32]. The FTIR spectra of some of the copolymers are given in Fig. 3.

In the PEO–TΦT and PPO–TΦT copolymers, the aramide crystalline carbonyl band was seen at 1647 $cm^{-1}$, the amorphous aramide at 1670–1680 $cm^{-1}$ and the ester carbonyl band at 1720 $cm^{-1}$. In the $PEO_{2000}$–TΦT system, the amorphous aramide band was visible at a lower wave number (1673 $cm^{-1}$) than for $PPO_{2200}$–TΦT (1678 $cm^{-1}$) and PTMO–TΦT (1684 $cm^{-1}$) [31,32]. A lower wave number of the amorphous carbonyl band suggests a stronger H-bonding in the amorphous phase, which might be due to either a clustering of the amide groups in the amorphous phase or an interaction with the polyether phase. However, if in fact an interaction took place between the polyether and the amide carbonyl band, then there should also occur an interaction with the ester carbonyl band. The peak position of the ester carbonyl band at 1720 $cm^{-1}$ did not change with the type of polyether.

It is also clear from Fig. 3 that the crystalline carbonyl peak (1645 $cm^{-1}$) was stronger for PPO–TΦT than for PEO–TΦT, suggesting that the TΦT crystallinities decreased with an increasing PEO concentration. From the intensities of the crystalline and the amorphous peaks, the TΦT crystallinity in the copolymers could be calculated according to Eq. (1) (Table 1). The TΦT crystallinities for the PPO–TΦT copolymers were high and little dependent on the type and length of the polyether.

### 3.4. AFM analysis

The morphology of the TΦT crystallites in $PEO_{1500}$–TΦT and the $PPO_{2200}$–TΦT was studied by AFM on cast film and without a heat treatment. The structure of the crystallites in cast films and bulk samples is often the same [37]. The micrographs of the $PEO_{1500}$–TΦT and the $PPO_{2200}$–TΦT copolymers are given in Fig. 4. The diamide segments in both materials were found to be represented by crystalline ribbons with high aspect ratios, as can be visualized in the figure.

A similar nano-ribbon structure of the TΦT crystallites has previously been observed for PTMO–TΦT [31,32,37]. Also with TEM such nano structures have been observed [33]. The extended length of the TΦT segment was approximately 2 nm. The long axis of the crystalline TΦT segments were oriented perpendicular to the ribbons' length axis. The micrograph of $PEO_{1500}$–TΦT seems less full which was possibly due to the lower TΦT crystallinity. The length

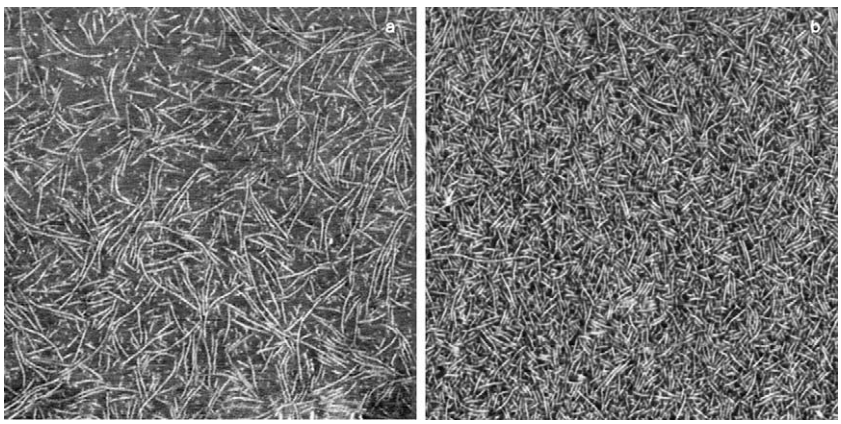


**Fig. 4.** AFM micrographs of (a) $PEO_{1500}$–TΦT and (b) $PPO_{2200}$–TΦT. The image size is 1 × 1 μm.

of the crystalline ribbons from merely the surface structures is difficult to determine as the crystallites bend out of the surface. It is often observed that when the crystalline concentration is lower the visible length of the crystallites is longer [37]. It was thus not possible to draw any conclusions regarding the total length of the crystalline ribbons from the obtained micrographs.

### 3.5. DMTA

The thermal mechanical properties were analyzed by DMTA, and Fig. 5 displays the storage modulus (G′) as a function of temperature for the nine copolymers, presented in three figures for the sake of clarity. The corresponding data are summarized in Table 1.

As can be observed in the DMTA graphs, three transitions were present: a glass transition of the polyether phase, a melting transition of the PEO crystallites and a melting transition of TΦT.

#### 3.5.1. $PEO_x$–TΦT

As can be seen in Fig. 5a, the $PEO_x$–TΦT copolymers had a $T_g$ of approximately −40 °C. At temperatures just above the $T_g$, the storage modulus of the $PEO_{1500}$ and $PEO_{2000}$ copolymers demonstrated a shoulder before the start of the rubbery plateau, which was due to the melting of the PEO crystallites. The shoulder height increased with the PEO segment length, suggesting an increased PEO crystallinity. The start of the rubbery plateau ($T_{flex}$) corresponded to the PEO melting temperatures as measured by DSC and was found to increase with an increasing PEO length (Table 1). The values of $T_{flex}$ for $PEO_{1500}$ and $PEO_{2000}$, were respectively, 25 and 35 °C, and at 20 °C these copolymers still had a PEO crystalline phase. As opposed to at 50 °C, their modulus at 20 °C was significantly higher as a result of the PEO crystalline phase (Table 1). The shorter $PEO_{1000}$ did not display a shoulder in the DMTA graph, suggesting that $PEO_{1000}$ segments had no or a very low crystallinity.

The shear modulus at the rubbery plateau was nearly constant with temperature. This behavior is typical for copolymers with monodisperse HS and is due to the fact that all the TΦT segments melt at the same temperature [12,24,27,28]. The rubber modulus was found to increase with the TΦT concentration (Table 1). The hard segments in the copolymers were phase separated by crystallization, and the functions of the nano-ribbon crystallites was twofold; they acted as physical crosslinks as well as reinforcing fillers [29,30]. The observed increase in modulus in the segmented block copolymers could be described by a fiber-reinforced composite model [24,28]. The modulus at the rubbery plateau (50 °C) increased considerably with the TΦT crystalline concentration as can be seen in Fig. 6.

The concentration of crystalline TΦT was calculated from the TΦT concentration and the TΦT crystallinity. Upon melting of the TΦT crystallites, the polymer started to flow and the flow transition temperatures ($T_{flow}$) decreased significantly with an increasing PEO segment length. This behavior is depicted in Fig. 7.

Pure TΦT units display a melting temperature of approximately 345 °C [38]. The HS melting temperature is known to decrease with increasing polyether concentration and increasing polyether–polyamide interaction, and this decrease has been explained as a result of the solvent effect of the polyether segments [12,24,27–29].

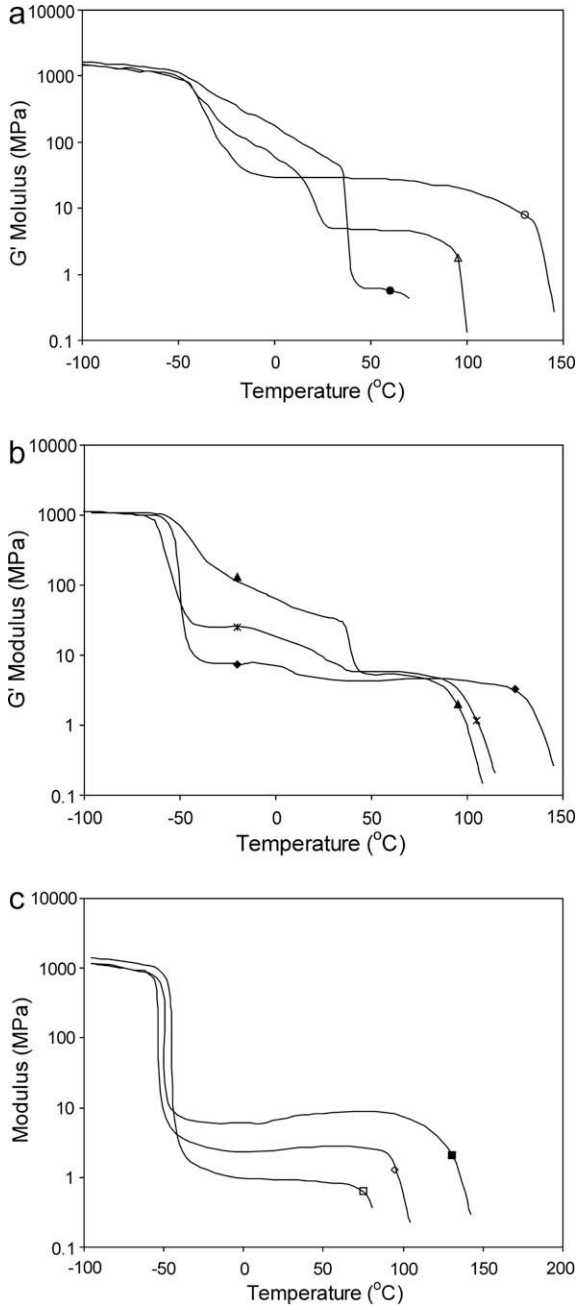


**Fig. 5.** The shear modulus as a function of temperature for (a) PEO, (b) PEO/PPO and (c) PPO: ○, $PEO_{1000}$; Δ, $PEO_{1500}$; ●, $PEO_{2000}$; ▲, $PEO_{2000}$/$PPO_{2200}$ (75/25); ✳, $PEO_{2000}$/$PPO_{2200}$ (50/50); ♦, $PEO_{2000}$/$PPO_{2200}$ (25/75); ■, $PPO_{2200}$; ◇, $PPO_{4200}$; □, $PPO_{6300}$.

#### 3.5.2. PPO–TΦT

Poly(propylene oxide) segments are known not to crystallize and this was also the case for the EO–PPO–EO segments [24]. The PPO–TΦT copolymers displayed two transitions: a $T_g$ for the PPO phase and a $T_m$ for the TΦT

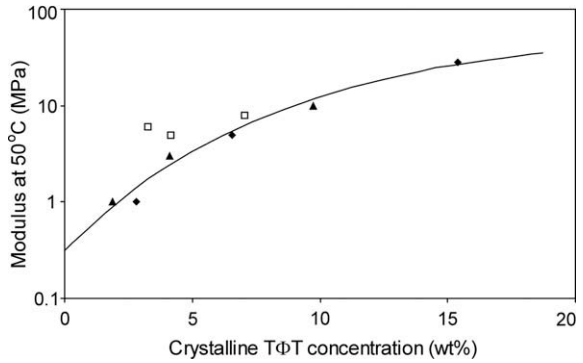


**Fig. 6.** The shear modulus as a function of the content of crystalline TΦT: ♦, PEO; ▲, PPO; □, PEO/PPO.

crystallites (Fig. 5c). The $T_g$ for the PPO phase was low (−48 to −59 °C) and the transitions sharp. As no crystalline polyether phase was present, the start of the rubbery plateau ($T_{flex}$) occurred at a very low-temperature (−45 to −48 °C), and these low values of $T_{flex}$, pointed at an excellent low-temperature flexibility of the PPO–TΦT copolymers. The $PPO_{6300}$–TΦT material seemed to display a slightly higher $T_g$ - a fact that remains unexplained. The shear modulus at the rubber plateau increased somewhat with increasing temperatures - a behavior typical of ideal elastomers and that has been observed earlier for segmented copolymers with monodisperse HS [12,24,27–29]. The shear modulus of the rubber plateau increased with increasing TΦT crystalline concentration (Fig. 6), and this increase was similar to that of the PEO–TΦT copolymers. The TΦT melting temperatures of the copolymers decreased with increasing PPO concentration (Fig. 7). It should, however, be mentioned that this decrease was not as significant as that for PEO, but stronger than for PTMO [29]. The effect of the type of polyether on the HS melting temperature has been explained to be the result of the changing interaction of the polyether and the amide segments [12]. Consequently, the interaction of the polyether with TΦT increased in the order of PTMO < PPO < PEO, thus confirming the trend described in the DSC section.

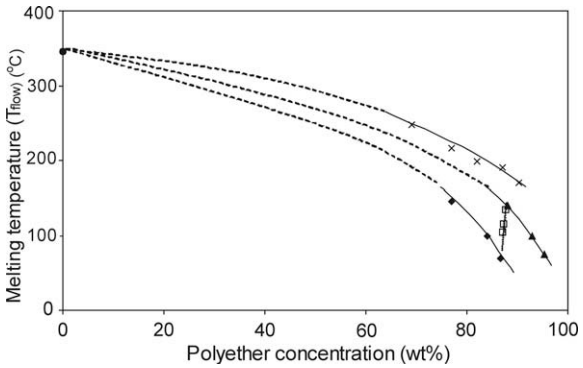


**Fig. 7.** The melting temperature of the TΦT segments in the copolymers as a function of the polyether segment concentration: ●, TΦT(neat) [38]; ♦, PEO; ▲, PPO; □, PEO/PPO; x, PTMO [31].

### 3.5.3. PEO/PPO–TΦT

In this series, the PEO/PPO segment ratio was varied while the TΦT concentration was kept constant. It can be seen in the DMTA graphs that the $T_g$ decreased gradually with an increasing PPO concentration from −41 to −60 °C (Fig. 5b). The $PEO_{2000}$ had a crystalline ether phase while $PPO_{2200}$ was amorphous. With an increasing PPO concentration, the shoulder of the PEO crystalline phase decreased in size and the copolymers with PEO/PPO ratios of 50/50 and 25/75 now demonstrated a shoulder that represented a separate and small transition.

Just as in the case of the TΦT crystallites, a linear decrease in the log modulus with the PEO crystallinity (PEO concentration) was expected. The modulus at the shoulder (−25 °C) decreased with decreasing $PEO_{2000}$ concentration, however, for the materials with ratios 50/50 and 25/75, the moduli were lower than expected (Fig. 8).

The above-mentioned results indicate that the PEO crystallinity decreased faster than what could be anticipated based on the composition. In accordance to what was described in the DSC section, it seemed that in the materials with ratios 50/50 and 25/75, the PEO segments displayed difficulties in crystallizing. Possibly, the PEO segments were dispersed in the PPO matrix. Moreover, the copolymers with PEO/PPO mixtures with ratios 50/50 and 25/75 maintained their low moduli down to low-temperatures. It could thus be concluded that even these PEO/PPO mixtures demonstrated decent low-temperature properties.

For PEO/PPO, the rubber modulus at 50 °C was slightly increased with an increasing PPO concentration (Table 1), however, if corrected for the TΦT crystallinity, as determined by FTIR, the PEO/PPO–TΦT copolymers were found to follow the general trend reasonably well (Fig. 6). The TΦT melting temperatures ($T_{flow}$) varied with the PEO concentration as expected (Fig. 7).

### 3.6. Water absorption

PEO segments are hydrophilic while PPO segments are more hydrophobic. By using mixtures of PEO and PPO, the hydrophilicity of the copolymers can be tuned. The water absorption of PEO copolymers was very high (64–125 wt.%) and increased significantly with an increasing PEO segment length (and thus also with an increasing

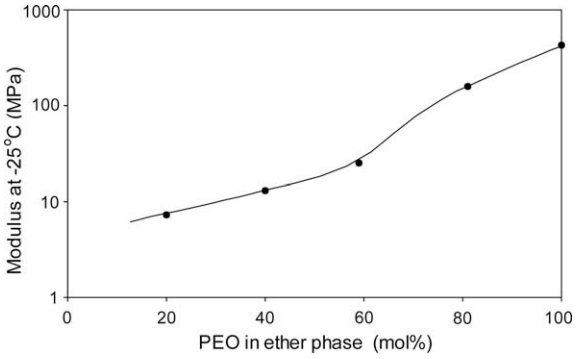


**Fig. 8.** The shear modulus at −25 °C as a function of the PEO concentration in the ether phase for the PEO/PPO mixtures.

PEO concentration and a decreasing TΦT concentration) (Table 1). The water absorption values based on the PEO segment length were higher than for the similar PEO–T6T6T copolymers [13], and this was believed to be due to the somewhat lower crystallinities of the TΦT segments as compared to those of T6T6T. For the copolymers with mixtures of PEO and PPO at an approximately constant TΦT concentration, the WA values increased linearly with the PEO concentration in the copolymer. This behavior is displayed in Fig. 9.

No synergistic effects were observed and it was thus concluded that the PPO did not interfere with the water absorption of the PEO segments. When varying the PEO concentration, the hydrophilicity of the segmented block copolymers could be modified.

## 4. Conclusions

Polyether–TΦT copolymers with varying amounts and segment lengths of PEO were studied. The PEO crystallinity and melting temperature were found to increase with the PEO segment length. When using mixtures of PEO/PPO, the polyether glass transition temperatures was observed to decrease with an increasing PPO concentration at the same time as which the PEO crystallinity was considerably reduced. The very low PEO crystallinities at low PEO segment concentrations suggest that the PEO segments might have been dispersed in the PPO phase. What consequence this might have on the surface and transport properties is as of yet unclear.

The TΦT segments crystallized into nano ribbons and the TΦT melting temperatures were found to decrease with the ether concentration. This decrease was a function of the polyether concentration as well as of the TΦT–polyether interaction. The latter seemed to increase according to PTMO > PPO > PEO. The moduli in the rubber plateau increased with the crystalline TΦT concentration, as expected. Moreover, the water absorption values increased with the polyether segment length, the PEO concentration and the decreasing TΦT concentration. When the polyether segment length and the TΦT concentrations were kept constant, the water absorption was found to increase linearly with the PEO concentration. The hydrophilicity of the polyether–TΦT copolymers could thus be readily varied by using mixtures of PEO and PEO–PPO–PEO segments. The hydrophilicity of the copolymers with mixtures of $PEO_{2000}$/$PPO_{2200}$–TΦT (50/50 and 25/75) compared well with that of $PEO_{1000}$–TΦT, and also displayed superior low-temperature properties.

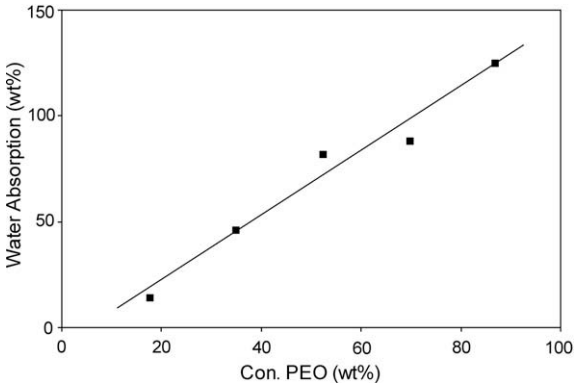


**Fig. 9.** The water absorption as a function of the PEO concentration in the ether phase for the PEO/PPO mixtures.

## Acknowledgements

Part of this research was financed by the Dutch Polymer Institute (DPI, The Netherlands), Project #497. The authors wish to express their gratitude to Mrs. H. ten Hoopen for performing the AFM analysis.

## References

[1] Holden G, Legge NR, Quirk PR, Schroeder HE. Thermoplastic elastomers. 2nd ed. Munich: Hanser Publishers; 1996.
[2] Fakirov S. Handbook of condensation thermoplastic elastomers. New York: Wiley; 2005.
[3] Schneider NS, Illinger JL, Karasz FE. Polymers of biological and biomedical significance. J App Polym Sci 1993;48:1723–9.
[4] Lee D, Lee S, Kim S, Char K, Park JH, Bae YH. Micro-phase-separation behavior of amphiphilic polyurethanes involving poly(ethylene oxide) and poly(tetramethylene oxide). J Polym Sci B Polym Phys 2003;41:2365–74.
[5] Chen CT, Eaton RF, Chang YJ, Tobolsky AV. Synthesis, characterization, and permeation properties of polyether-based polyurethanes. J Appl Polym Sci 1972;16:2105–14.
[6] Yilgör I, Yilgör E. Hydrophilic polyurethaneurea membranes: influence of soft block composition on the water vapor permeation rates. Polymer 1999;40:5575–81.
[7] Gebben B. A water vapor-permeable membrane from block copolymers of poly(butylene terephthalate) and polyethylene oxide. J Membr Sci 1996;113:323–9.
[8] Stroeks A, Dijkstra K. Modelling the moisture vapour transmission rate through segmented block co-poly(ether–ester) based breathable films. Polymer 2001;42:117–27.
[9] Metz SJ, Mulder MHV, Wessling M. Gas-permeation properties of poly(ethylene oxide) poly(butylene terephthalate) block copolymers. Macromolecules 2004;37:4590–7.
[10] Bondar VI, Freeman BD, Pinnau I. Gas sorption and characterization of poly(ether-*b*-amide) segmented block copolymers. J Polym Sci B Polym Phys 1999;37:2463–75.
[11] Bondar VI, Freeman BD, Pinnau I. Gas transport properties of poly(ether-*b*-amide) segmented block copolymers. J Polym Sci B Polym Phys 2000;38:2051–62.
[12] Husken D, Feijen J, Gaymans RJ. Hydrophilic segmented block copolymers based on poly(ethylene oxide) and monodisperse amide segments. J Polym Sci A Polym Chem Ed 2007;45:4522–35.
[13] Husken D, Gaymans RJ. The structure of water in PEO-based segmented block copolymers and its effect on transition temperatures. Macromol Chem Phys 2008;209:967–79.
[14] Deschamps AA, Grijpma DW, Feijen J. Poly(ethylene oxide)/poly(butylene terephthalate) segmented block copolymers: the effect of copolymer composition on physical properties and degradation behavior. Polymer 2001;42:9335–45.
[15] Husken D, Feijen J, Gaymans RJ. Surface properties of poly(ethylene oxide)-based segmented block copolymers with monodisperse hard segments. J Appl Polym Sci 2009;114:1264–9.
[16] Husken D, Gaymans RJ. Water vapor transmission of poly(ethylene oxide)-based segmented block copolymers. J Appl Polym Sci 2009;112:2143–50.
[17] Husken D, Visser T, Wessling M, Gaymans RJ. $CO_2$ permeation properties of poly(ethylene oxide)-based segmented block copolymers. J Membr Sci, submitted for publication.
[18] Rault J, Le Huy HM. Polyamide–polyether block copolymers swollen by water. I. Properties. J Macromol Sci Phys 1996;35:89–114.
[19] Husken D, Gaymans RJ. The tensile properties of poly(ethylene oxide)-based segmented block copolymers in the dry and wet state. J Mater Sci 2009;44:2656–64.
[20] Park JH, Bae YH. Hydrogels based on poly(ethylene oxide) and poly(tetramethylene oxide) or poly(dimethyl siloxane). II. Physical properties and bacterial adhesion. J Appl Polym Sci 2003;89:1505–14.

[21] Park JH, Cho YW, Kwon IC, Jeong SY, Bae YH. Assessment of PEO/PTMO multiblock copolymer/segmented polyurethane blends as coating materials for urinary catheters: in vitro bacterial adhesion and encrustation behavior. Biomaterials 2002;23:3991–4000.
[22] Shibaya M, Suzuki Y, Doro M, Ishihara H, Yoshihara N, Enomoto M. Effect of soft segment component on moisture-permeable polyurethane films. J Polym Sci B Polym Phys 2006;44:573–83.
[23] Husken D, Feijen J, Gaymans RJ. Synthesis and properties of segmented block copolymers based on mixtures of poly(ethylene oxide) and poly(tetramethylene oxide) segments. Eur Polym J 2008;44:130–43.
[24] Van der Schuur JM, Gaymans RJ. Segmented Block copolymers based on poly(propylene oxide) and mono disperse polyamide-6,T segments. J Polym Sci A Polym Chem Ed 2006;44:4769–81.
[25] Harrell LL. Segmented Polyurethans. Properties as a function of segment size and distribution. Macromolecules 1969;2:607–12.
[26] Miller JA, Lin SB, Hwang KKS, Wu KS, Gibson PE, Cooper SL. Properties of polyether–polyurethane block copolymers: effects of hard segment length distribution. Macromolecules 1985;18:32–44.
[27] Krijgsman J, Gaymans RJ. Tensile and elastic properties of thermoplastic elastomers based on PTMO and tetra-amide units. Polymer 2004;45:437–46.
[28] Biemond GJE, Feijen J, Gaymans RJ. Poly(ether amide) segmented block copolymers with adipic acid based tetraamide segments. J Appl Polym Sci 2007;105:951–63.
[29] Niesten MCEJ, Feijen J, Gaymans RJ. Synthesis and Properties of segmented copolymers having aramid units of uniform length. Polymer 2000;41:8487–500.
[30] Niesten MCEJ, Harkema S, Van Der Heide E, Gaymans RJ. Structural changes of segmented copolyesteramides of uniform aramid units induced by melting and deformation. Polymer 2001;42:1131–42.
[31] Arun A, Gaymans RJ. Segmented block copolymers with monodisperse aramide end-segments. Macromol Chem Phys 2008;209:854–63.
[32] Arun A, Dullaert K, Gaymans RJ. Structure and properties of mono-, di-, tri- and multi-block segmented copolymers with diamide hard segments. Macromol Chem Phys 2009;210:48–59.
[33] Garcia JM, De La Campa JG, De Abajo J. Aliphatic–aromatic poly(ether amides)s containing oxyethelene units. Synthesis and characterization. J Polym Sci A 1996;34:659–67.
[34] Garcia JM, Alvarez JC, De La Campa JG, De Abajo J. Thermal behavior of aliphatic–aromatic poly(ether-amides)s. J App Polym Sci 1997;67:975–81.
[35] König HM, Gorelik T, Kolb U, Kilbinger AFM. Supramolecular PEG-co-oligo(*p*-benzamide)s prepared on a peptide synthesizer. J Am Chem Soc 2007;129:704–8.
[36] Schleuss TW, Schollmeyer D, Kilbinger AFM. A precursor route to supramolecular oligo(*p*-phenylene terephthalamide block copolymers. Macromol Rapid Commun 2008;29:293–8.
[37] Sauer BB, McLean RS, Gaymans RJ, Niesten MCEJ. Crystalline morphologies in segmented copolymers with hard segments of uniform length. J Polym Sci B Polym Phys 2004;42:1783–92.
[38] Gaymans RJ, Harkema S. Melting behavior of aliphatic and aromatic diamides. J Polym Sci B Polym Phys 1977;15:587–90.